International Journal of Power Electronics and Drive Systems (IJPEDS)
Vol. 14, No. 4, December 2023, pp. 2094~2106
ISSN: 2088-8694, DOI: 10.11591/ijpeds.v14.i4.pp2094-2106

Comparison of control strategies for thermoelectric generator emulator

Razman Ayop, Chee Wei Tan, Shahrin Md Ayob, Mohd Zaki Daud, Jasrul Jamani Jamian, Norjulia Mohamad Nordin
Department of Electrical Power Engineering, Faculty of Electrical Engineering, Universiti Teknologi Malaysia, Johor Bahru, Malaysia

Article Info

Article history:

Received Feb 8, 2023
Revised Apr 30, 2023
Accepted May 7, 2023

Keywords:

Buck converter
Emulator
Peltier device
PI controller
TEG

ABSTRACT

Thermoelectric generator (TEG) can directly convert heat energy into electrical energy. It improves the power efficiency of the energy generation system by converting the power loss in the form of heat produced during the generation process into additional electrical energy. The TEG emulator (TEGE) is a power converter that produces a similar current-voltage characteristic as the TEG. It is a valuable device used to develop and test the TEG-based energy generation system. Nonetheless, the research on the TEGE is still in the early stage. This paper proposed a proper, low-cost, and high-efficient TEGE design using the buck converter. The contribution of the paper covers the TEG model in the form of an array, the buck converter design tailored to the TEGE, and 4 new control strategies proposed for the TEGE. The control strategies are the direct referencing method (DRM), perturb and observed (PnO) method, resistance comparison method (RCM), and resistance feedback method (RFM). The conventional proportional-integral controller is used to maintain a smooth operation during transient and steady-state periods. The results show the merits or demerits for each proposed control strategy based on the accuracy, transient response, stability, overshoot, and efficiency.

Corresponding Author:

Razman Ayop
Department of Electrical Power Engineering, Faculty of Electrical Engineering
Universiti Teknologi Malaysia
81310, UTM Johor Bahru, Johor, Malaysia
Email: razman.ayop@utm.my

1. INTRODUCTION

A thermoelectric generator (TEG) or Peltier device is a module that is able to change heat energy to electrical energy directly. The device consists of two sites, the hot and cold sites. The larger the temperature difference between these sites, the higher the output power produced [1]. The current-voltage (I-V) characteristic curve of a TEG module is also not linear, similar to the photovoltaic (PV) module. Nonetheless, the I-V characteristic for the TEG is simpler compared to the PV module. Therefore, the maximum power point tracking (MPPT) algorithm is needed to ensure all the power produced by the TEG module is extracted [2], [3].

During the operation of the PV module, the temperature of the PV module increases resulting in power loss in the form of heat. Several researchers have proposed to hybridize the TEG with the PV module [4]–[6]. This allows the power loss produced to be converted into usable electrical energy. The TEG modules are commonly placed at the back of the PV module, which has a higher temperature compared to the ambient temperature. Due to the temperature difference between the PV module and the air, the power is generated from the TEG. The result from the research shows that there are power increases up to 58% for the

hybrid PV-TEG system when compared to the standard PV system [6]. Besides placing the TEG modules at the back of the PV module, there is also another method that transfer the heat away from the PV module to the TEG modules to further improve the efficiency of the system [7]. Besides PV, the TEG technology is also being implemented in the nuclear auxiliary power and biogas [8]. Therefore, the TEG module is a useful technology that can convert the power loss in the form of heat into useful electrical energy.

In the power electronics field, an emulator is a power supply that generate a specific I-V characteristic. The conventional power supply commonly produces a constant voltage or constant current. However, an emulator voltage and current is not constant and commonly depends on the load. The emulator is commonly used during the development of a product or the testing of the system. The advantages of using the emulator instead of actual components are commonly small in size, highly efficient, lower in cost, safer alternative, easy to configure, and able to repeat the condition of the test. These emulators include the PV emulator [9], [10], wind turbine emulator [11], battery emulator [12], and load emulator (also known as electronic load) [13]. Nonetheless, the research conducted on the TEG emulator (TEGE) is still in the early stage. The current TEGE uses a commercial PV emulator to emulate the I-V characteristic curve of a TEG [14]. Although this approach is applicable, the cost for the conventional PV emulator is high. A proper, low-cost, and high-efficient TEGE design is needed to allow a more convenient development and testing process of the TEG generation system. Therefore, the control strategies from PV emulator is adopted into the TEGE since both PV emulator and TEGE produce same DC output.

The first control strategy available from the PV emulator is the direct referencing method (DRM) [15], [16]. This control strategy is common due to the simple implementation process. It uses the transient response of the closed-loop controller and power converter to determine the operating point of an emulator. Nonetheless, it is susceptible to the changes in the transient response. Since the load change affects the transient response, it can lead to oscillating problem. The perturb and observe (PnO) control strategy for the emulator is based on the common MPPT algorithm [17]. It is based on a fixed step size to determine the operating point of an emulator. As a result, it produces large oscillation similar to the MPPT if the step size is not properly tuned. The resistance comparison method (RCM) is another control strategy available in emulator [18], [19]. Instead of using continuously calculating the operating point like the DRM and PnO, the RCM calculating the operating point first before producing the reference input. It allows a more stable emulation. However, the processing burden is high. The resistance feedback method (RFM) is similar to RCM, with lower computation burden [9], [20]. Nevertheless, the model needs to be mathematically modified.

This paper proposed the TEGEs using the buck converter. There are four control strategies proposed for the TEGE (adopted from the PV emulator) and the control strategies are simulated individually. The array TEG model has been proposed for a higher power application in the TEGE. The modified design of the buck converter is also proposed to fit the TEGE application for maintaining the continuous current mode operation and at a specific output voltage ripple. The standard proportional-integral (PI) controller is applied for the TEGE. The paper is based on the simulation using MATLAB/Simulink. The simulation results are designed to prove the derivation of the buck converter and the performance of the proposed control strategies. The next section proposed the design of the TEGE. Section 3 shows the results and discussions. The latter section deduces the finding from the simulation.

2. PROPOSED DESIGN FOR THERMOELECTRIC GENERATOR EMULATOR

The TEGE consists of four main components, which is the TEG model, power converter, closed-loop controller for the power converter, and control strategy. The power converter used for the TEGE is the buck converter. While the closed-loop controller used for the TEGE is the PI controller.

2.1. Thermoelectric generator array model

The TEG mathematical model for a single module is shown in (1) [1], [21]. The power produced for a single TEG module is low and it is not suitable for power generation. Therefore, the modules need to be connected in the series and parallel connection, as shown in Figure 1. Assume each TEG receive the same temperature and has the same $S_{teg(u)}$, ΔT, and $R_{int(u)}$. Using Thevenin Theorem, the Thevenin resistance, R_{th}, is derived and shown in (2). By applying the Kirchhoff current law at the V_{teg}, the derivation becomes in (3). The Thevenin voltage, Vth, which is also the open-circuit voltage, Voc, is derived from in (4) to become (4). By applying the Kirchhoff voltage law, Vteg becomes in (5). By substituting in (2) and (4) into (5), the TEG model array is shown in (6).

$$V_{teg(u)} = S_{teg(u)}\Delta T - I_{teg(u)}R_{int(u)} \quad (1)$$

$$R_{th} = R_{int} = \frac{N_{ser}R_{int(u)}}{N_{par}} \quad (2)$$

$$\frac{N_{par}\left(V_{th}-N_{ser}S_{teg(u)}\Delta T\right)}{N_{ser}R_{int(u)}}=0 \quad (3)$$

$$V_{th}=V_{oc}=N_{ser}S_{teg(u)}\Delta T \quad (4)$$

$$V_{teg}=V_{th}-I_{teg}R_{th} \quad (5)$$

$$V_{teg}=N_{ser}S_{teg(u)}\Delta T-\frac{N_{ser}}{N_{par}}I_{teg}R_{int(u)} \quad (6)$$

Where $V_{teg(u)}$ is the voltage of a TEG module, $S_{teg(u)}$ is the see beck coefficient of a TEG module, ΔT is the temperature difference between the hot and cold sites ($\Delta T=T_h-T_l$), T_h is the temperature at hot site, T_l is the temperature at cold site, $I_{teg(u)}$ is the current of a TEG module, $R_{int(u)}$ is the internal resistance of a TEG module, and N_{ser} is the number of TEGs in series and N_{par} is the number of TEGs in parallel.

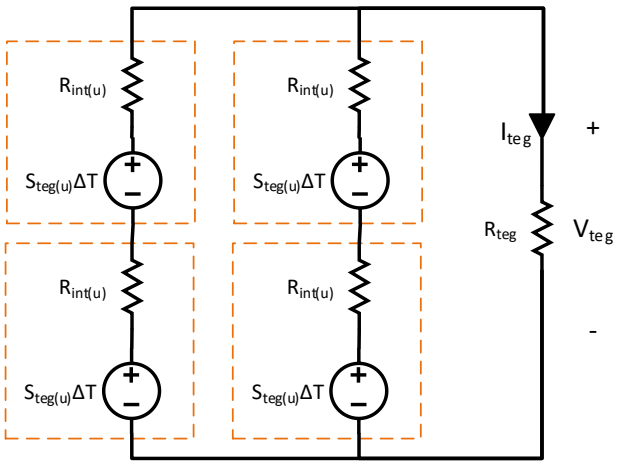

Figure 1. The equivalent circuit of the TEGs connected in series and parallel

2.2. Buck converter design

When it comes to emulator applications, the buck converter shines as it can handle various tasks effectively while maintaining a minimal component count. These components are the power switch, diode, inductor, and capacitor, as presented in Figure 2. When designing a buck converter, three parameters need to be considered, which are the duty cycle (D), continuous current mode operation, and the output voltage ripple. The design for the buck converter is widely known [22]. Nonetheless, these designs not consider the dynamic operation of an emulator. Therefore, the conventional buck converter is modified to suit the TEGE.

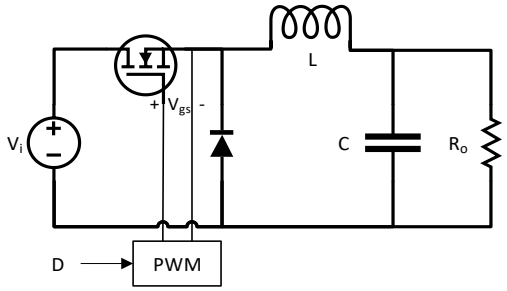

Figure 2. The equivalent circuit of the buck converter

The input voltage, V_i, is based on the V_{oc} of the PV array at the highest temperate difference of th TEG, ΔT_{max}. Therefore, the V_i is calculated using (7). Since the D relates to R_o for the TEGE, the minimum

and maximum R_o ($R_{o(min)}$ and $R_{o(max)}$, respectively) need to be calculated based on the minimum and maximum D (D_{min} and D_{max}, respectively). For MPPT application, the $R_{o(min)}$ and $R_{o(max)}$ is consistent based on the maximum power point theory, which is shown in (8).

$$V_i = N_{ser} S_{teg(u)} \Delta T_{max} \tag{7}$$

$$R_{o(max)} = R_{o(min)} = \frac{N_{ser} R_{int(u)}}{N_{par}} \tag{8}$$

For emulation purposes, the range of emulation is based on D_{min} and D_{max}. To relate the D with R_o, the TEG model is modified. In (9) is substituted into (6) and produces (10). Since the $R_{o(max)}$ occurs at D_{max}, (10) is modified to become (11), which the assumption is the requirement of the $R_{o(max)}$ occur when the ΔT is at maximum. The D_{max} is calculated based on (12). Therefore, the $R_{o(max)}$ is calculated using (13). Using the same approach, the $R_{o(min)}$ is calculated using (14).

$$I_{teg} = \frac{V_{teg}}{R_{teg}} \tag{9}$$

$$R_o = \frac{N_{ser} R_{int(u)} V_{teg}}{N_{par}\left(N_{ser} S_{teg(u)} \Delta \mathrm{T} - V_{teg}\right)} \tag{10}$$

$$R_{o(max)} = \frac{N_{ser} R_{int(u)} V_{teg(max)}}{N_{par}\left(N_{ser} S_{teg(u)} \Delta T_{max} - V_{teg(max)}\right)} \tag{11}$$

$$V_{teg(max)} = D_{max} N_{ser} S_{teg(u)} \Delta T_{max} \tag{12}$$

$$R_{o(max)} = \frac{N_{ser} R_{int(u)} D_{max}}{N_{par}(1 - D_{max})} \tag{13}$$

$$R_{o(min)} = \frac{N_{ser} R_{int(u)} D_{min}}{N_{par}(1 - D_{min})} \tag{14}$$

Maintaining the continuous current mode hinges on the precise choice of inductance, L. Based on the conventional buck converter design, the L required to maintain the continuous current mode is shown in (15). The output voltage ripple is maintained by choosing the right capacitance, C. Based on the conventional buck converter design, the C required to maintain the output voltage ripple is shown in (16).

$$L \geq \frac{(1 - D_{max}) R_{o(max)}}{2 f_s} \tag{15}$$

$$C \geq \frac{(1 - D_{min})}{8 L \gamma_{Vo} {f_s}^2} \tag{16}$$

Where f_s is the switching frequency and γ_{Vo} is the output voltage ripple factor.

2.3. Proportional integral controller

Commonly, an emulator requires a closed-loop controller for the power converter used within the emulator. This applies to the TEGE. Due to its prevalent usage in emulator applications, the PI controller is selected as the preferred option. This is due to the simplicity of the PI controller (G_{pi}), as shown in (17), and the availability of the transfer function for the buck converter (G_{buck}), as shown in (18) [23], [24]. The arrangement of the G_{pi} and G_{buck} is shown in Figure 3. The proportional and integral gains, K_p and K_i, respectively, are tuned automatically using the single input single output (SISO) tool available in MATLAB.

$$G_{pi}(s) = K_p + \frac{K_i}{s} \tag{17}$$

$$G_{buck}(s) = \frac{\hat{d}}{\hat{v}_o} = \frac{{}^{V_i}/_{LC}}{s^2 + {}^{1}/_{R_o C} s + {}^{1}/_{LC}} \tag{18}$$

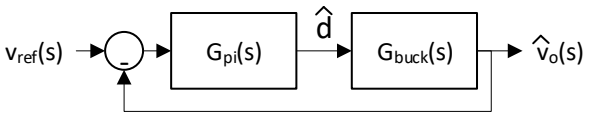

Figure 3. The block diagram of the closed-loop buck converter with PI controller

2.4. Control strategies

The main purpose of the control strategy is to pinpoint the appropriate operating point for the TEGE. Four control strategies are proposed, which are the DRM, PnO, RCM, and RFM. The TEG model, PI controller, and buck converter is kept constant for all control strategies.

2.4.1. Direct referencing method

The DRM is a simple control strategy that uses the transient response of the TEGE to determine the operating point. This control strategy is adopted from the common control strategy used in the PV emulator [15], [16]. The I_o is measured and fed into the TEG model, as shown in Figure 4. The TEG model produces the reference voltage, V_{ref}, and it is compared with the V_o before going to the PI controller. The PI controller determines the D for the buck converter. The process is repeated until the V_{ref} is equal to V_o.

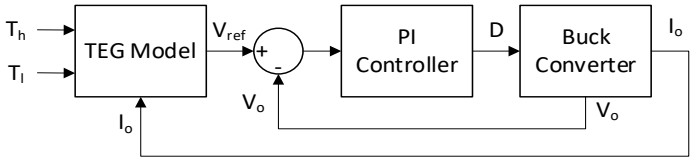

Figure 4. The block diagram of the DRM

2.4.2. Perturb and observe method

The PnO uses fixed step sizes instead of relying fully on the transient response of the TEGE. This is expected to be a more robust control strategy when compared to the DRM while maintaining its simplicity. The PnO is adopted from the common MPPT algorithm used in the PV generation application [25]. The I_o is measured and fed into the PnO, as shown in Figure 5(a). The I_o is used to determine the V_{teg}, as shown in Figure 5(b). The V_{teg} is compared with the V_o. If V_{teg} is larger than V_o, the V_{ref} is increased with a fixed step size called the perturbation voltage, V_{per}. If V_{teg} is smaller than V_o, the V_{ref} is decreased with a fixed step size of V_{per}. The V_{ref} is compared with the V_o and the difference is fed into the PI controller. The PI controller determines the D for the buck converter. The process is repeated until the V_{ref} is equal to V_o. The V_{per} and perturbation time (t_{per}) are 0.1 V and 30 µs, respectively.

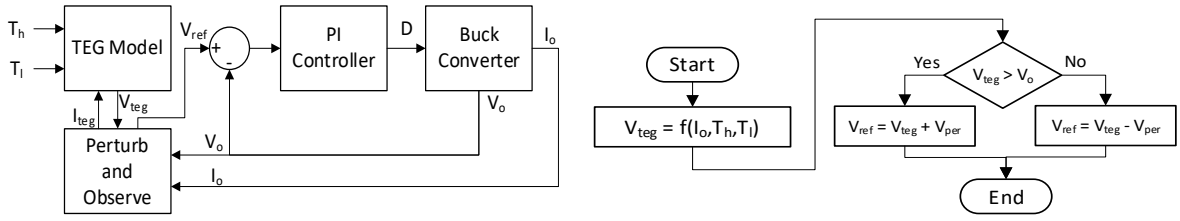

(a) (b)

Figure 5. The PnO: (a) block diagram and (b) flowchart

2.4.3. Resistance comparison method

The RCM uses both V_o and I_o to determine the operating point. As a result, the Vref produced is expected to be more stable compared to the DRM and PnO. The RCM is modified from the RCM obtained from the PV emulator that uses an integral controller to determine the operating point [19], [26], [27]. The process starts by measuring the V_o and I_o. Then the R_o is digitally calculated by dividing V_o with the I_o. As the

result, the R_o is determined instantaneously. However, the TEG model only has current and not resistance as the input. Therefore, the integral controller is used to convert the resistance input into the current input. The R_o is compared with the TEG resistance, R_{teg}, by dividing the V_{teg} with the I_{teg}, as shown in Figure 6. The difference is fed into an integral controller with RCM gain, K_{rcm}. The K_{rcm} is adjusted based on the response of the TEGE using the try and error method. The V_{ref} is obtained from the V_{teg} at a much faster rate. Therefore, the operating point is produced before the transient period of the TEGE ended. of the TEGE is completed. This is expected to produce a more robust control strategy. The PI controller receives input from both V_{ref} and V_o, comparing them to compute the error. The PI controller determines the D for the buck converter. The process is repeated until the V_{ref} is equal to V_o.

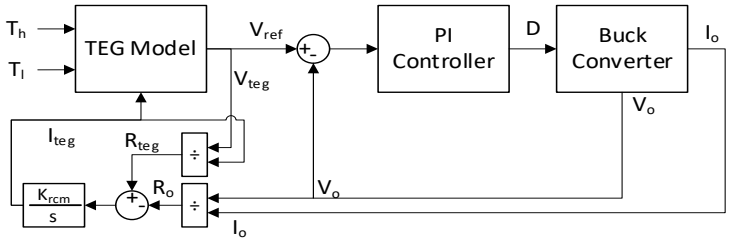

Figure 6. The block diagram of the RCM

2.4.4. Resistance feedback method

The RFM uses both V_o and I_o as the feedback, similar to the RCM. Nevertheless, the RFM has the simplicity of the DRM. Unfortunately, it requires a modification of the TEG model. The control strategy is adopted from the PV emulator [20]. The process starts by changing the I_{teg} input of the TEG model using Ohm's Law, as shown in (9). In (9) is substituted into (6) and produces (19). This new TEG model has R_{teg} as the input. Referring to Figure 7, the V_o and I_o are measured and the R_o is digitally calculated. Using the modified TEG model, the V_{ref} is instantaneously calculated. The V_{ref} is compared with the V_o and the difference is fed into the PI controller. The PI controller determines the D for the buck converter. The process is repeated until the V_{ref} is equal to V_o.

$$V_{teg} = \frac{N_{ser} S_{teg(u)} \Delta T}{\frac{N_{ser}}{N_{par}} \frac{R_{int(u)}}{R_{teg}} + 1} \quad (19)$$

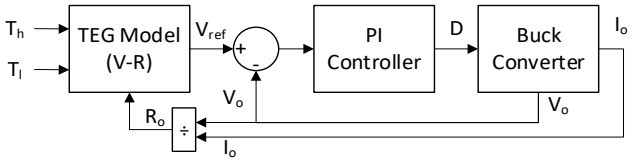

Figure 7. The block diagram of the RFM

3. RESULTS AND DISCUSSIONS

The results and discussions consist of two parts that cover two proposed designs. The first analysis is conducted to determine the accuracy of the buck converter design for the TEGE application. While the second part analyses the performance of the control strategies. The control strategies are simulated with various R_o ranging from 1 Ω to 85 Ω. The T_h and T_l are kept at 100 °C and 30 °C, respectively. The temperature changes are not analyzed for this paper.

3.1. Design analysis of buck converter for thermoelectric generator emulator

The analysis of the buck converter for the TEGE focuses on the duty cycle, continuous current mode operation, and output voltage ripple factor. If the derivation is accurate, the simulation follows the design specification of the buck converter for the TEGE. This means that the duty cycle is between the minimum and maximum value. While the current at the inductor don't become zero during steady state condition. Lastly, the output voltage ripple factor doesn't go above the desired value.

3.1.1. Duty cycle

When designing the emulator, the R_o relates to the D. If the R_o is not properly calculated, the D can be out of the range between D_{min} and D_{max}. Therefore, it is essential to calculate the $R_{o(min)}$ and $R_{o(max)}$. The design specification for the D_{min} and D_{max} is 0.1 and 0.9, respectively. Based on this specification, the $R_{o(min)}$ and $R_{o(max)}$ are 1 Ω to 85 Ω, respectively. The simulated D is shown in Figure 8. The result shows that all the TEGEs maintain its operation within the boundary of the D. Therefore, the derived (13) and (14) is accurate. Note that the D is slightly higher for $R_{o(min)}$ and $R_{o(max)}$ due to the effect of the nonideality of various components in the buck converter.

3.1.2. Continuous current mode

Ensuring continuous current mode operation is crucial in the design of the buck converter. If the buck converter switches to discontinuous current mode, it alters the transfer function, necessitating a distinct type of PI controller. Consequently, to ensure proper design of the PI controller, it is imperative to maintain continuous current mode in the buck converter consistently. This is done by a proper design of L using (15). The continuous current mode operation in the simulation is observed using the minimum inductor current, $I_{L(min)}$, which never goes to zero. Based on the result in Figure 9, the $I_{L(min)}$ never goes to zero. This indicates that the derived (15) is accurate. The $I_{L(min)}$ becomes smaller as R_o increases.

3.1.3. Output voltage ripple

The output voltage ripple is controlled by choosing the right C. The C is calculated using (16). The output voltage ripple is measured using the γ_{Vo}, and is calculated using (20). Based on the derived (16), the highest γ_{Vo} should occur when the $R_{o(min)}$ is connected, which the TEGE operates at D_{min}. However, the simulation result does not follow the design, as shown in Figure 10. The maximum γ_{Vo} should be 1%, yet it is only 0.41% only. This shows that the derived equation produces an overdesign buck converter for the TEGE. Although this considers following the design parameter, the overdesign results in slower transient response. Therefore, a more accurate design is needed for the C of the buck converter used in the TEGE application.

$$\gamma_{Vo} = \frac{(V_{o(max)} - V_{o(min)})}{V_o} \times 100\% \quad (20)$$

Where $V_{o(max)}$ is the maximum output voltage and $V_{o(min)}$ is the minimum output voltage

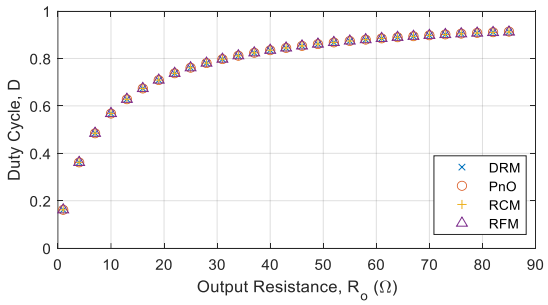

Figure 8. The D against R_o

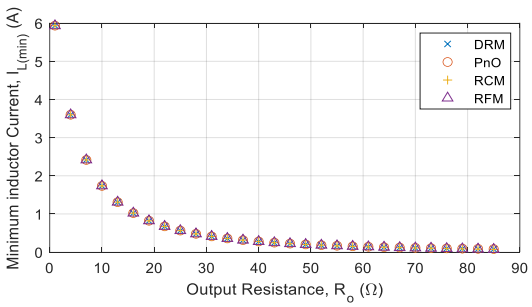

Figure 9. The $I_{L\ (min)}$ against R_o

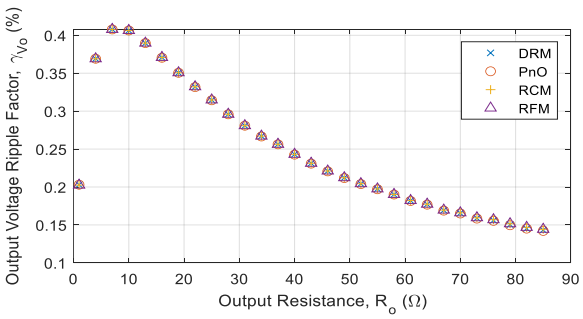

Figure 10. The γ_{Vo} against R_o

3.2. Performance analysis for control strategies

The performance analysis of the proposed control strategies for the TEGE focuses on the accuracy, transient response, operating point stability, percentage overshoot, and efficiency. This analysis shows the advantages and disadvantages of the proposed control strategies. A good control strategy should have high accuracy, fast transient response, stable operating point, low or no overshoot, and high efficiency.

3.2.1. Accuracy

Accuracy plays a pivotal role in emulator applications, and it encompasses three types of analysis: emulator accuracy, model accuracy, and control strategy accuracy. In the case of the TEGE, the emulator accuracy assesses the conformity between the TEGE's output and the TEG array's output. The model accuracy evaluates the alignment between the TEG model and the TEG array. Lastly, the control strategy accuracy compares the TEGE's output with the TEG model. As the paper's main focus revolves around control strategies, the accuracy of the control strategy is utilized to evaluate the precision of the proposed TEGE. The accuracy of the TEGE is analysed using the percentage voltage error, $e_{\%v}$, which is calculated based on the TEGE voltage (V_{tege}) and the voltage of the TEG model (V_{tegm}), as shown in (21). The lower the $e_{\%v}$, the higher the accuracy.

$$e_{\%v} = \frac{|V_{tege} - V_{tegm}|}{V_{tegm}} \times 100\% \quad (21)$$

The results in Figure 11 show that the accuracy of the DRM is higher compared to other control strategies. However, the accuracy of the DRM changes with R_o. The $e_{\%v}$ is low around 0.0004% when the load is 31 Ω and 68 Ω. However, the accuracy becomes lower when the R_o is at the minimum and maximum limit, which the $e_{\%v}$ is around 0.5%. This irregular change inaccuracy is due to the dependency of the DRM on the other components in the TEGE, such as the buck converter, PI controller, and TEG model. For this particular design specification, the accuracy produced is high. Nevertheless, the accuracy changes with the different design specifications. The PnO, RCM, and RFM don't depend on external components like the DRM. Therefore, the accuracy is almost similar even the R_o changes, which is around 0.02% to 0.04%. In conclusion, the PnO, RCM, and RFM have consistent accuracy. While the accuracy of the DRM depends on the parameters of the components used in the TEG.

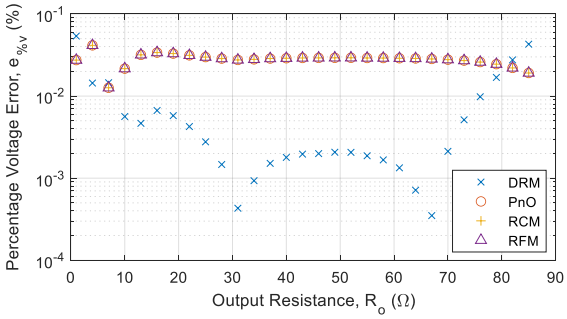

Figure 11. The $e_{\%v}$ against R_o

3.2.2. Transient response

The transient response is an important aspect of the TEGE. The TEG array has a fast response. However, this fast response cannot be emulated since the buck converter is used. This is because both converters contain L and C that result in a slow transient response. The response can be improved by choosing a higher f_s. Still, the computation time for the digital controller in the TEGE may not be compatible if the buck converter is too fast. Therefore, a suitable f_s needs to be chosen if the hardware is implemented. For this paper, this relationship is not considered. The transient response of the TEGE is measured using the settling time, T_s. The T_s is the time taken for the V_o to be within 2% of its final values. The T_s during start-up is simulated and recorded in Figure 12.

The results show that the DRM and PnO has similar T_s at various R_o. While the RCM and RFM show similar almost similar T_s at various R_o. The DRM and PnO have faster responses compared to the RCM and RFM. This is due to the characteristic of the V_{ref} during the transient period. For the DRM and PnO, when the TEGE starts, the I_o is low. The I_o is fed into the TEG model. When the TEG model receives a low I_o during the transient period, the TEG model produces a high V_{ref}, as shown in Figure 13(a). This high V_{ref}

produces a fast response by the PI controller, which result in a lower T_s. As the TEGE comes closer to the steady-state, the I_o increases, and the V_{ref} decreases. This characteristic of the V_{ref} allows a faster transient response. However, this characteristic also affects the performance of the PI controller. The properly tuned PI controller may become unstable. The design of the PI controller is also affected by this characteristic. Although the RCM and RFM have a slower response compared to the DRM and PnO, the V_{ref} produces is consistent, as shown in Figure 13(b), and it does not affect the design of the PI controller. In conclusion, DRM and PnO are faster compared to RCM and RFM, but affect the design of the PI controller. The RCM and RFM don't affect the design of the PI controller.

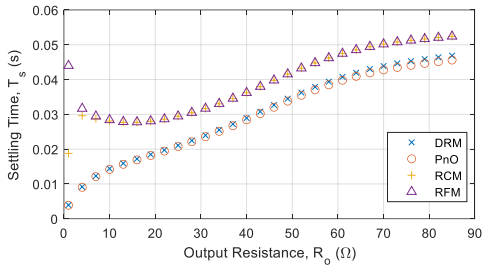

Figure 12. The T_s against R_o

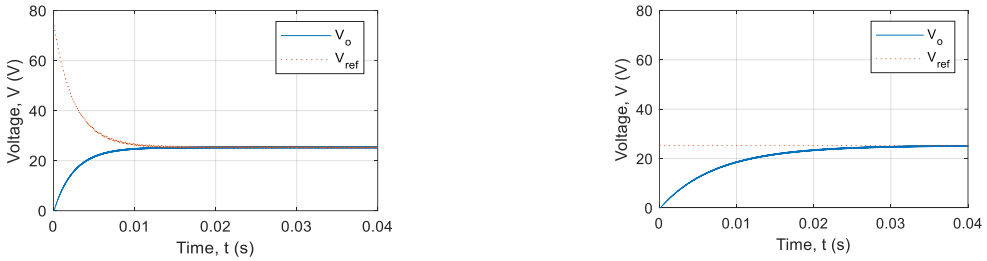

Figure 13. The V_o and V_{ref} against time at R_o of 5 Ω, (a) DRM and (b) RFM

3.2.3. Operating point stability

The stability of the operating point is the ability of the control strategy to maintain a stable reference input for the TEGE. The stability of the operating point is analyzed using the reference voltage ripple factor, γ_{Vref}, which is calculated using (22). The higher the γ_{Vref}, the more unstable the operating point, which leads to unstable TEGE. A good control strategy has γ_{Vref} that equal to 0%, which can be considered as a robust control strategy.

$$\gamma_{Vref} = \frac{|V_{ref(max)} - V_{ref(min)}|}{V_{ref}} \times 100\% \quad (22)$$

Where $V_{ref(max)}$ is the maximum reference voltage and $V_{ref(min)}$ is the minimum reference voltage in one period of the buck converter switching operation.

The advantage of using both V_o and I_o as the feedback for the TEG is that the operating point can be determined instantaneously, which result in 0% γ_{Vref} displayed in Figure 14. Therefore, the operating point is stable. This means that there is no need to focus on the other component affecting the performance of the TEGE. On the other hand, the DRM and PnO have high γ_{Vref}, especially when the R_o is low (1.36% γ_{Vref}). The DRM determines the operating point of the TEGE by measuring the I_o only. Based on the I_o, the V_{ref} is calculated based on the TEG model. Since the buck converter is used, the I_o contain ripples. These ripples result in unstable operating points. Since the ripple is higher at lower R_o for buck converter, the γ_{Vref} becomes higher at low R_o. The PnO also produce a high γ_{Vref} since it also used the I_o as the feedback. The γ_{Vref} (1.58%) is higher when compared to the DRM since the PnO uses a fixed step size. Nonetheless, the PnO algorithm response is slower compared to DRM, which does not result in an unstable emulation. In conclusion, the RCM and RFM produce a stable operating point. While, the operating point for the DRM and PnO has high γ_{Vref}, especially when the γ_{Vref} is low.

3.2.4. Percentage overshoot

The PI controller for the TEGE is designed to operate in optimally damped conditions. This means that the transient response of the buck converter is the fastest without any V_o overshoot occurring during start-up. Some of the control strategies disturb the PI controller design that causes the overshoot to occur. Therefore, this analysis is essential to determine the robustness of the control strategies. The overshoot is measured using the percentage overshoot, %OS, and it is calculated using (23).

$$\%OS = \frac{|V_{o(max)} - V_o|}{V_o} \times 100\% \quad (23)$$

The results presented in Figure 15 shows that the RCM and RFM do not produce any overshoot. This shows that these control strategies do not disturb the PI controller operation, thus, making these control strategies a more robust choice. The DRM produce a high %OS of 0.08% when the R_o is 1 Ω. Nevertheless, the %OS decreases as the R_o increases. This effect is caused by the significant increases in the V_{ref} during the start-up, which results the overshoot. The effect is less as the R_o increases because there is no significant increase in V_{ref} as the R_o increases. The overshoot in the PnO is around 0.03% and it is nearly consistent for all R_o. The overshoot is caused by the fixed step size used in the PnO. This can be improved by using a smaller step size. However, this leads to slower transient response.

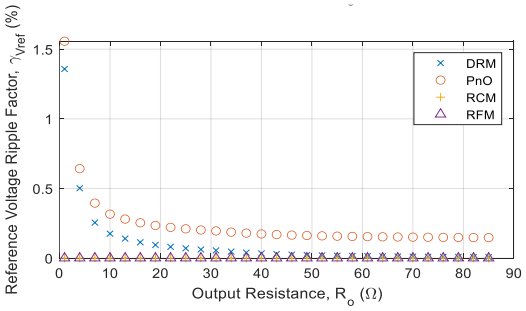

Figure 14. The γ_{Vref} against R_o

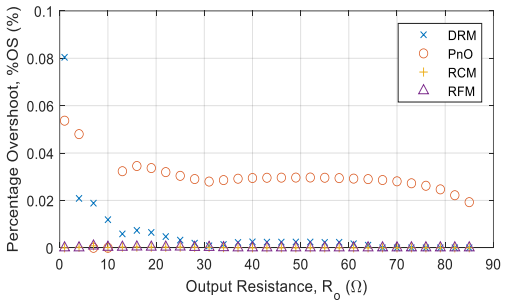

Figure 15. The $\%OS$ against R_o

3.2.5. Efficiency

The efficiency is one of the performances that need to be analyzed for the TEGE. A good TEGE should has high efficiency. The efficiency of the TEGE, η, is calculated using (24). The η for various control strategies and at various R_o is shown in Figure 16. The results show that the control strategies do not affect the η. This is because all four control strategies show similar η. Based on the results, the η is low when the R_o is low. As the R_o increases, the η increases up to 96%. The η is low when the R_o is low because the I_o is high during that condition. As the result, the I_i and the inductor current (I_L) is also high. Since there is resistance at the MOSFET and inductor, power loss occurs at these components. Since the current is high, the power loss is significant, thus producing a lower η:

$$\eta = \frac{V_o I_o}{V_i I_i} \times 100\% \quad (24)$$

where I_i is the input current.

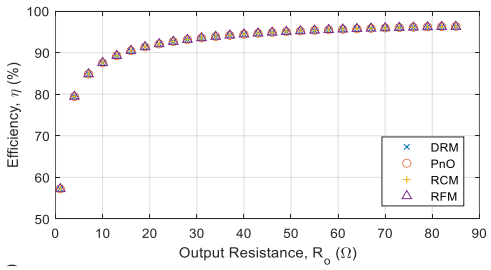

Figure 16. The η against R_o

3.2.6. Performance summary

The performance of the control strategy is summaries in Table 1. If an accurate TEGE is needed, the DRM should be implemented. The high accuracy is caused by the variable step sizes produce by the DRM. The DRM and P&O has faster response compared to the RCM and RFM, even though the PI controller used is the same. However, the DRM and P&O produce oscillating operating point and high overshoot. While the RCM and RFM produce a stable operating point and a no overshoot. The result shows that the efficiency remain the same for all control strategies. This means that the efficiency does not affect by the control strategies. However, it is shown that the efficiency is low when the R_o is low. At this condition, the current passing through the components in the buck converter is high, which result in a high-power loss.

Table 1. The performance of the control strategies

Control strategy	DRM	P&O	RCM	RFM
Accuracy	High	Low	Low	Low
Transient response	Fast	Fast	Slow	Slow
Operating point stability	Oscillate	Oscillate at low R_o	Stable	Stable
Percentage overshoot	High at low R_o	High	No overshoot	No overshoot
Efficiency	Low at low R_o	Low at low R_o	Low at low R_o	Low at low R_o

4. CONCLUSION

This research aim is to propose a proper, low-cost, and high-efficient design of a TEGE using the buck converter. The objectives of the research include the TEG model in the form of an array, the buck converter design specific to the TEGE application, and the control strategies. The TEG array has been derived using the Thevenin Theory. The buck converter design has been proved to operate within the duty cycle limit and in the continuous current model. Nonetheless, the derivation of the capacitance required to maintain the output voltage ripple needs to be improved. For accuracy, the proposed DRM has high accuracy. However, the accuracy is inconsistent. The proposed DRM and PnO has a faster transient response when compared to the proposed RCM and RFM. Nevertheless, the RCM and RFM has better operating point stability and has no overshoot compared to the DRM and PnO. The research also concludes that the control strategy does not affect the efficiency of the TEGE. In conclusion, a proper, low-cost, and high-efficient design of a TEGE using the buck converter has been proposed together with four new control strategies for the TEGE.

ACKNOWLEDGEMENTS

This research was supported by Ministry of Higher Education (MOHE) through Fundamental Research Grant Scheme (FRGS/1/2021/TK0/UTM/02/19). The authors would like to express gratitude to University Technology Malaysia (UTM) for providing comprehensive facilities. Lastly, thanks to colleagues who have either directly or indirectly contributed to the completion of this work.

REFERENCES

[1] N. P. Bayendang, M. T. E. Kahn, V. Balyan, I. Draganov, and S. Pasupathi, "A comprehensive thermoelectric generator (TEG) modelling," *AIUE Proceedings of the Energy and Human Habitat Conference*, 2020.

[2] A. Belkaid, I. Colak, K. Kayisli, R. Bayindir, and H. I. Bulbul, "Maximum power extraction from a photovoltaic panel and a thermoelectric generator constituting a hybrid electrical generation system," *6th IEEE International Conference on Smart Grid, icSmartGrids 2018*, pp. 276–282, 2019, doi: 10.1109/ISGWCP.2018.8634534.

[3] M. Ruzaimi Ariffin, S. Shafie, W. Z. W. Hassan, N. Azis, and M. Effendy Ya'Acob, "Conceptual design of hybrid photovoltaic-thermoelectric generator (PV/TEG) for Automated Greenhouse system," *IEEE Student Conference on Research and Development: Inspiring Technology for Humanity, SCOReD 2017 - Proceedings*, vol. 2018-January, pp. 309–314, 2018, doi: 10.1109/SCORED.2017.8305373.

[4] R. Bjørk and K. K. Nielsen, "The performance of a combined solar photovoltaic (PV) and thermoelectric generator (TEG) system," *Solar Energy*, vol. 120, pp. 187–194, 2015, doi: 10.1016/j.solener.2015.07.035.

[5] C. Babu and P. Ponnambalam, "The theoretical performance evaluation of hybrid PV-TEG system," *Energy Conversion and Management*, vol. 173, pp. 450–460, 2018, doi: 10.1016/j.enconman.2018.07.104.

[6] S. Koushik, S. Das, V. Sharma, P. Walde, and N. Maji, "PV and TEG hybrid power generation for enhancement of efficiency," *India International Conference on Power Electronics, IICPE*, vol. 2018-December, 2018, doi: 10.1109/IICPE.2018.8709422.

[7] Z. Song, J. Ji, J. Cai, Z. Li, and Y. Gao, "Performance prediction on a novel solar assisted heat pump with hybrid Fresnel PV plus TEG evaporator," *Energy Conversion and Management*, vol. 210, 2020, doi: 10.1016/j.enconman.2020.112651.

[8] W. He, G. Zhang, X. Zhang, J. Ji, G. Li, and X. Zhao, "Recent development and application of thermoelectric generator and cooler," *Applied Energy*, vol. 143, pp. 1–25, 2015, doi: 10.1016/j.apenergy.2014.12.075.

[9] R. Ayop, C. W. Tan, and K. Y. Lau, "Computation of current-resistance photovoltaic model using reverse triangular number for photovoltaic emulator application," *Indonesian Journal of Electrical Engineering and Informatics*, vol. 7, no. 2, pp. 314–322, 2019, doi: 10.11591/ijeei.v7i2.1148.

[10] R. Ayop and C. W. Tan, "An adaptive controller for photovoltaic emulator using artificial neural network," *Indonesian Journal of Electrical Engineering and Computer Science*, vol. 5, no. 3, pp. 556–563, 2017, doi: 10.11591/ijeecs.v5.i3.pp556-563.
[11] D. Zouheyr, B. Lotfi, and B. Abdelmadjid, "Improved hardware implementation of a TSR based MPPT algorithm for a low cost connected wind turbine emulator under unbalanced wind speeds," *Energy*, vol. 232, 2021, doi: 10.1016/j.energy.2021.121039.
[12] M. Zauner, P. Mandl, C. Hametner, O. Konig, and S. Jakubek, "Flatness-based discrete-time control of a battery emulator driving a constant power load," *IEEE Journal of Emerging and Selected Topics in Power Electronics*, vol. 9, no. 6, pp. 6864–6874, 2021, doi: 10.1109/JESTPE.2021.3059917.
[13] R. Ayop, S. M. Ayob, C. W. Tan, T. Sutikno, and M. J. A. Aziz, "Comparison of electronic load using linear regulator and boost converter," *International Journal of Power Electronics and Drive Systems*, vol. 12, no. 3, pp. 1720–1728, 2021, doi: 10.11591/ijpeds.v12.i3.pp1720-1728.
[14] E. A. Man, D. Sera, L. Mathe, E. Schaltz, and L. Rosendahl, "Thermoelectric generator emulator for MPPT testing," in *2015 Intl Aegean Conference on Electrical Machines & Power Electronics (ACEMP), 2015 Intl Conference on Optimization of Electrical & Electronic Equipment (OPTIM) & 2015 Intl Symposium on Advanced Electromechanical Motion Systems (ELECTROMOTION)*, Sep. 2015, pp. 774–778. doi: 10.1109/OPTIM.2015.7427051.
[15] S. Esfandiari, S. H. Montazeri, and J. Milimonfared, "Improvement of a high-accuracy photovoltaic emulator by considering wind effect," *11th Power Electronics, Drive Systems, and Technologies Conference, PEDSTC*, 2020, doi: 10.1109/PEDSTC49159.2020.9088354.
[16] D. S. and R. Thabit, "A new low cost solar array emulator based on fuzzy and 32-bit microcontroller," *International Journal of Science and Engineering Investigations*, vol. 9, no. 101, pp. 63–69, 2020.
[17] O. Ozden, Y. Duru, S. Zengin, and M. Boztepe, "Design and implementation of programmable PV simulator," *2016 International Symposium on Fundamentals of Electrical Engineering, ISFEE 2016*, 2016, doi: 10.1109/ISFEE.2016.7803229.
[18] D. Chariag and L. Sbita, "Design and simulation of photovoltaic emulator," *International Conference on Green Energy and Conversion Systems, GECS 2017*, 2017, doi: 10.1109/GECS.2017.8066121.
[19] R. Ayop, C. W. Tan, and C. S. Lim, "The resistance comparison method using integral controller for photovoltaic emulator," *International Journal of Power Electronics and Drive Systems*, vol. 9, no. 2, pp. 820–828, 2018, doi: 10.11591/ijpeds.v9.i2.pp820-828.
[20] R. Ayop, C. W. Tan, and A. L. Bukar, "Simple and fast computation photovoltaic emulator using shift controller," *IET Renewable Power Generation*, vol. 14, no. 11, pp. 2017–2026, 2020, doi: 10.1049/iet-rpg.2019.1504.
[21] A. Makki, S. Omer, Y. Su, and H. Sabir, "Numerical investigation of heat pipe-based photovoltaic-thermoelectric generator (HP-PV/TEG) hybrid system," *Energy Conversion and Management*, vol. 112, pp. 274–287, 2016, doi: 10.1016/j.enconman.2015.12.069.
[22] D. W. Hart, "Power electronics," Valparaiso University, Indiana: Tata McGraw-Hill Education, 2011.
[23] M. Alaoui, H. Maker, A. Mouhsen, and H. Hihi, "Real-time emulation of photovoltaic energy using adaptive state feedback control," *SN Applied Sciences*, vol. 2, no. 3, 2020, doi: 10.1007/s42452-020-2294-2.
[24] S. E. I. Remache, A. Y. Cherif, and K. Barra, "Optimal cascaded predictive control for photovoltaic systems: Application based on predictive emulator," *IET Renewable Power Generation*, vol. 13, no. 15, pp. 2740–2751, 2019, doi: 10.1049/iet-rpg.2019.0068.
[25] R. Alik and A. Jusoh, "An enhanced P&O checking algorithm MPPT for high tracking efficiency of partially shaded PV module," *Solar Energy*, vol. 163, pp. 570–580, 2018, doi: 10.1016/j.solener.2017.12.050.
[26] O. López-Santos, M. C. Merchán Riveros, M. C. Salas Castaño, W. A. Londoño, and G. Garcia, "Emulation of a photovoltaic module using a wiener-type nonlinear impedance controller for tracking of the operation point," *Communications in Computer and Information Science*, vol. 742, pp. 482–494, 2017, doi: 10.1007/978-3-319-66963-2_43.
[27] I. D. G. Jayawardana, C. N. M. Ho, M. Pokharel, and G. Escobar, "A fast dynamic photovoltaic simulator with Instantaneous Output Impedance Matching controller," *2017 IEEE Energy Conversion Congress and Exposition, ECCE 2017*, vol. 2017-January, pp. 5126–5132, 2017, doi: 10.1109/ECCE.2017.8096863.

BIOGRAPHIES OF AUTHORS

Razman Ayop received the bachelor's degree in electrical engineering with first-class honours, the master's degree in electrical engineering with specialization in power system, and the PhD degree in electrical engineering from Universiti Teknologi Malaysia (UTM), Johor, Malaysia, in 2013, 2015, and 2018, respectively. He is a Senior Lecturer with UTM and a member of Power Electronics and Drives Research Group, Faculty of Electrical Engineering, UTM. He is also the Executive Committee for IEEE Malaysia Power Electronics Society (PELS) Chapter in 2021 & 2022. His research interests include renewable energy and power electronics. This includes the photovoltaic (PV) emulator, maximum power point tracking (MPPT) converter, standalone energy management and sizing, PV modelling, vehicle to grid (V2G) system, particle swarm optimization, and fuzzy logic controller. He can be contacted at email: razman.ayop@utm.my.

Chee Wei Tan received his B.Eng. degree in Electrical Engineering (First Class Honors) from Universiti Teknologi Malaysia (UTM), in 2003 and a Ph.D. degree in Electrical Engineering from Imperial College London, London, U.K., in 2008. He is currently an associate professor at Universiti Teknologi Malaysia and a member of the Power Electronics and Drives Research Group, Faculty of Electrical Engineering. His research interests include the application of power electronics in renewable/alternative energy systems, control of power electronics and energy management system in microgrids. He is also a Chartered Engineer registered with Engineering Council, UK, a professional engineer registered with Board of Engineers Malaysia and a professional technologist registered with Malaysia Board of Technologists. He was awarded the Malaysia Research Start Award (High Impact Paper – Engineering and Technologies) 2018 by the Ministry of Education Malaysia. He can be contacted at email: cheewei@utm.my.

Shahrin Md Ayob was born in Kuala Lumpur, Malaysia. He obtained his first degree in Electrical Engineering, Master in Electrical Engineering (Power), and Doctor of Philosophy (Ph.D.) from Universiti Teknologi Malaysia in 2001, 2003, and 2009, respectively. Currently, he is an associate professor at the Faculty of Electrical Engineering, Universiti Teknologi Malaysia. He is a registered Graduate Engineer under the Board of Engineer Malaysia (BEM) and Senior Member of IEEE. His current research interest is the solar photovoltaic system, electric vehicle technology, fuzzy system, and evolutionary algorithms for power electronics applications. He can be contacted at email: e-shahrin@utm.my.

Mohd Zaki Daud is a Lecturer at Faculty of Electrical Engineering, Universiti Teknologi Malaysia since 1997. He received his BEng in Electrical Engineering from University of Southampton, UK in 1995 and M.Sc. in Electric Power from University of Newcastle upon Tyne in 1997. Currently he is embarking a Ph.D. in Electrical Engineering. His current research interest includes harmonics in power electronics-based power system, estimation techniques in electric drives, modelling of electromagnetic processes using soft computing techniques, renewable energy and engineering education. He can be contacted at email: mdzaki@utm.my.

Jasrul Jamani Jamian received the Bachelor of Engineering (B. Eng. (Hons)) degree, Master of Engineering (M. Eng.) and Ph.D degree in electrical (power) engineering from Universiti Teknologi Malaysia in 2008, 2010 and 2013 respectively. He is actively involved in research as a principal investigator as well as leader in consultancy projects with several companies such as Petronas and Tenaga Nasional Berhad, which focuses on relay coordination projects and off grid solar PV design. His research interest includes network reconfiguration, optimization technique, and renewable energy. He can be contacted at email: jasrul@utm.my.

Norjulia Mohamad Nordin received her degree in bachelor of electrical engineering from the Universiti Teknologi Malaysia (UTM) in 2006 and the Master in Engineering Science from the University of New South Wales in 2008. She then received her Ph.D in electrical engineering from UTM in 2016. Currently, she is a Senior Lecturer at the Faculty of Engineering, Universiti Teknologi Malaysia (UTM). Her current research interests are in AC motor drives/electrical drives, power electronics applications, electrical machines and renewable energy conversion. She can be contacted at email: norjulia@utm.my.